Very slow surfactant adsorption at the solid–liquid interface is due to long lived surface aggregates†

Shaun C. Howard and Vincent S. J. Craig*

Received 23rd February 2009, Accepted 22nd May 2009
First published as an Advance Article on the web 25th June 2009
DOI: 10.1039/b903768c

Until recently it was believed that surfactant adsorption was completed very rapidly, but now it is understood that following the initial rapid adsorption of surfactant a much slower adsorption process can continue for many hours. Adsorption isotherms for cetyltrimethylammonium bromide (CTAB) on silica have been measured using optical reflectometry (OR) in the absence and presence of 1 mM and 10 mM KBr. Adsorption from bulk concentrations ranging from 0.3 to 1 × cmc showed evidence of slow adsorption, casting some doubt on the true value of equilibrium surface excess for these concentrations. To further explore this effect a series of concentration cycling (ziggurat) experiments were performed using both OR and a quartz crystal microbalance (QCM), these serve to highlight the disparity between surface excesses determined *via* concentration and dilution experiments. A mechanism for slow adsorption is proposed whereby the absence of collisions for adsorbed aggregates removes the dominant mode of equilibration, which therefore proceeds slowly by monomer adsorption. The proposed mechanism should apply equally to all types of surfactant, suggesting that slow adsorption is a universal phenomenon.

Introduction

The adsorption of surfactants at the solid–water interface is important for the control of wetting, lubrication, detergency and in mineral flotation. Historically the adsorption process has been inferred from equilibrium measurements of surfactant surface excess.[1–3] These measurements and wetting studies have led to the recognition that surface adsorbed aggregates are formed and that the amount of surfactant adsorbed (the surface excess) is intimately related to the structure of the adsorbing aggregates, though the precise nature of the aggregates, particularly at low surface coverage, remains unclear. On hydrophobic surfaces, the chains of the surfactant are attracted to the substrate and the adsorption proceeds 'tail first' up until monolayer coverage.[4] On hydrophilic surfaces, the adsorption of an oppositely charged ionic surfactant is thought to initially be driven by electrostatic interactions. At higher bulk concentrations bilayered aggregates or admicelles are formed.[5] The prevailing view has been that between these two limits asymmetrical aggregates with the head groups facing the substrate, termed hemimicelles, are present, this is known as the four-region model for the isotherm.[3] Recent evidence has shown that for CTAB on silica, bilayered aggregates dominate throughout the adsorption isotherm (this is consistent with the two-step model of the isotherm[1] and hemimicelles are absent and the presence or absence of a hemimicellar regime is dependent upon the balance between electrostatic and hydrophobic interactions).[6]

Above the critical surface aggregation concentration (csac), where the surface excess reaches a maximum, an array of surfactant aggregate structures have been observed using atomic force microscopy (AFM).[7–9] At concentrations below the csac it is extremely difficult to image aggregates due to an insufficiently repulsive interaction force (*i.e.* they are too soft). The morphology of the aggregates is influenced by the substrate and different substrates have different templating powers. For all surfactants on HOPG and for cationic surfactants on mica the crystal structure strongly controls the type of aggregates and the ordering on the surface.[9,10] Whereas the templating effect with amorphous silica is far weaker, such that the adsorbed structures on a silica surface reflect those present at moderately higher concentrations in the bulk.[11]

In this work we are interested not only in how the adsorbed structures influence the surface excess but also in how the adsorbed structures influence the adsorption kinetics. Until recently it was believed that surfactant adsorption was completed very rapidly, in which case these issues would be moot, but now it is understood that following the initial rapid adsorption of surfactant a much slower adsorption process can continue for many hours and it is thought that this process is intimately related to the nature of the aggregates present on the surface.[5,12] Aided by improvements in instrumental sensitivity, it is our aim to explore these relationships.

The prevailing convention has been that micelles rapidly exchange with monomers in the bulk solution and that this leads to rapid equilibration between micelles and monomers. In contrast, the process of equilibration between the surface and the solution at times proceeds very slowly. Prior to the direct measurements of slow surfactant adsorption[12,13] there existed

Department of Applied Mathematics, Research School of Physics and Engineering, Australian National University, Canberra, ACT 0200, Australia. E-mail: vince.craig@anu.edu.au

† Electronic supplementary information (ESI) available: Concentration cycling experiment using both OR and QCM for CTAB in the absence of electrolyte as shown in Fig. 11 but without baseline correction. See DOI: 10.1039/b903768c.

indirect evidence of this slow adsorption. When surface force measurements are made between surfaces with adsorbed cationic surfactants it is routine to allow the surfaces to equilibrate for long periods (12 h or more) as the force required to displace surface bound surfactant increases over this time period.[14] From later experiments, using AFM to image surfactant aggregates, it was found that higher quality images were often obtained after 30 min of equilibration time[7] and the force required to push through the adsorbed surfactant layers increased, suggesting that the aggregates had become more ordered and robust. Further, the very fact that such aggregates can routinely be imaged using AFM and that the morphology is repeatable from one image to the next indicates that such aggregates are not labile and remain unchanged on the scale of minutes. We believe the fact that equilibration is very slow is directly due to the longevity of surface adsorbed aggregates and we explore below why surface adsorbed aggregates are long lived.

Materials and methods

Cetyltrimethylammonium bromide (CTAB) (purity greater than 99%) was obtained from Aldrich, recrystallised twice from acetone and freeze–dried prior to use. KBr (Analytical Grade, 99.9+%) was obtained from Aldrich and used as received. All water used was filtered and passed through a Millipore Gradient filtration unit before use. The surface tension of the water at room temperature was measured regularly by the pendant drop technique (KSV) and found to be ~73.0 mN m^{-1}. The critical micelle concentration (cmc) for each system (0.89 mM (no salt), 0.75 mM (1 mM KBr) and 0.13 mM (10 mM KBr)) was determined from the break in the surface tension data plotted against the log of concentration using data obtained *via* the pendant drop method (KSV CAM-300, Finland). No minima were found in the surface tension data around the cmc, indicating no gross contamination.

Silicon wafers with a well defined 319 nm oxide layer were used in all studies (Silicon Valley Microelectronics, CA). Surfaces with low hydroxyl group density are obtained upon baking due to condensation reactions at the silica surface that results in the formation of siloxane bonds.[15] The remaining hydroxyl groups are isolated and therefore less likely to participate in hydrogen bonded stabilisation of hydronium ions at the surface.[15] In solution, these hydroxyl groups are therefore more acidic and the silica surface will be more highly charged. Silica of this type is known as pyrogenic. Pyrogenic silica will slowly rehydroxylate when immersed in water resulting in hydroxylated silica. In this work, the initially pyrogenic silica was cleaned with piranha solution (H_2O_2 80% w/w; 20% w/w HNO_3) for <30 s, rinsed with water, soaked in 10% w/w NaOH for <30 s and stored in water until use. This process ensured that the silica surface was fully hydroxylated without altering the thickness of the oxide layer. Immediately before use the surfaces were rinsed with water and distilled ethanol before being dried under a dry nitrogen stream. The thickness of the oxide layer present on the silicon wafer was determined ellipsometrically to be 319 ± 2 nm (Beaglehole instruments).

The optical reflectometry (OR) technique follows that used by Djit *et al.*[16] and is shown schematically in Fig. 1. Briefly, OR relies upon changes in the reflective properties of a substrate that occur upon adsorption of the species of interest. In order to

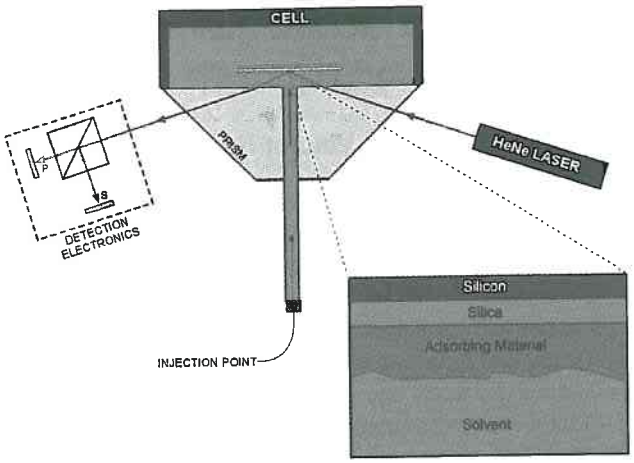

Fig. 1 Schematic of an optical reflectometer. A beam of polarised light from a HeNe laser is reflected from the surface of interest and the p and s components of the reflected light are converted to a voltage at the detector. Upon adsorption of material the intensity of the reflected p and s components is altered and a four-layer optical model allows this signal to be converted to adsorbed surface excess according to eqn (1).

convert changes in optical properties to surface excess an optical model is required to calculate the sensitivity parameter which is used to convert changes in the polarisation of reflected light to a measure of surface excess. The sensitivity parameter A_s was determined to be -0.024 m^2 mg^{-1} for our experiments from a four-layer Fresnel optical model solved using the matrix method of Abelès,[17] taking the refractive indices of water, silica and silicon as 1.333, 1.46 and 3.80, respectively, and using a dn/dC value for the surfactant of 0.149 cm^3 g^{-1}.[18,19] The water and silicon layers are treated as semi-infinite and the thickness of the silica layer was 319 nm. In a typical reflectometry experiment the cell initially contains only solvent (in this case water or the relevant salt solution) while a stable baseline is recorded. Baseline data obtained using KBr solutions without the presence of CTAB were very stable, this indicated the lack of absorbing contaminants present in the salt. Surfactant is then passed into the cell *via* a two-way valve and the change in the ratio of the two perpendicular polarisations of the laser beam recorded, which is proportional to the surface excess according to:

$$\Gamma = \frac{\Delta S}{S_0 A_S} \quad (1)$$

where Γ is the adsorbed surface excess, S_0 is the baseline ratio of the reflectivities of the p and s components, *i.e.* $S_0 = R_p/R_s$ (usually ~1), ΔS is the change in polarisation and A_S is the sensitivity parameter obtained from the optical model. We note that the technique measures the amount of surfactant adsorbed at the surface and is insensitive to the conformation of material at the interface. Therefore any change in signal measured is due to a change in the amount of material at the interface as opposed to a structural change of that material. For this work a customised reflectometer was constructed to minimise electronic noise, maximise temperature stability and optimise data acquisition rates. The reflectometer is entirely contained in an incubator, in a temperature controlled room allowing the temperature to be accurately maintained at 23 °C ± 0.1 °C. Instrument stability was generally found to be better than 0.02 mg m^{-2} and data were

generally discarded if the baseline drift exceeded 0.05 mg m^{-2} over the duration of the experiment.

QCM (KSV Z500, Finland) measurements were performed using 5 MHz AT-cut quartz crystals with a silica coating. QCM is commonly employed to follow the adsorption of surfactants, particles, polymers and proteins to a substrate.[20–25] The change in resonant frequency (Δf) of the crystal can be related to the adsorbed amount (Δm) using the Sauerbrey equation,[26] which is known to perform well for films that behave elastically:

$$\Delta m = -\frac{\rho_q l_q}{f_0}\frac{\Delta f}{n} = -C_{QCM}\frac{\Delta f}{n} \quad (2)$$

where f_0 is the fundamental frequency, n is the overtone number, ρ_q and l_q are the specific density and thickness of the quartz crystal, respectively. C_{QCM} (17.7 ng cm^{-2} Hz^{-1} for our crystals) is the mass sensitivity constant. In the case of adsorbed surfactant, the mass calculated using the Sauerbrey equation, hereafter called the Sauerbrey mass, includes a contribution due to the mass of entrained water in the film and therefore adsorbed amounts determined by QCM routinely exceed adsorbed amounts determined by other methods.[27] The degree of solvent coupling can be determined by use of deuterated solvents,[28] or comparison with other measurements of surface excess. Crystals were thoroughly rinsed with water and distilled ethanol before being subjected to RF water plasma cleaning at 30 W for less than 1 min. Freshly cleaned crystals were used immediately. A steady baseline was obtained for at least 30 min prior to starting the experiment.

In the present study, all the results reported are from the frequency shift in the third overtone ($n = 3$) and were conducted at 23 ± 0.1 °C. The third overtone is preferred over the fundamental overtone as the resonator is less affected by mechanical forces associated with mounting the resonator. Noise levels and baseline drift were not as stable as that obtained with the optical reflectometer, reflecting differences in the quality of the data obtainable with the two instruments. The use of QCM was particularly interesting as we wished to determine if the shear wave influenced the slow adsorption of surfactant in any way.

Results and discussion

In a typical OR experiment solvent is flowing into the cell during the acquisition of a baseline signal. The same fluid with the addition of surfactant is then introduced and the change in polarisation of the reflected signal over time recorded. At a later time the flow is switched back to the solvent alone and the adsorbed surfactant is washed from the surface. The polarisation data are converted into a surface excess using eqn (1) either during or following the experiment. Typical data for the adsorption of CTAB in the absence and presence of electrolyte are presented in Fig. 2. The solutions shown are 0.3 mM CTAB without salt, in 1 mM KBr and in 10 mM KBr. The general form of the adsorption data was consistent for all surfactant and electrolyte concentrations. Before the introduction of surfactant, a baseline was first recorded using the solvent; in this case, either water, 1 mM KBr or 10 mM KBr. Surfactant was then passed into the cell at 100–120 s resulting in a rapid increase in the surface excess. The surface excess remained relatively constant whilst surfactant solution was flowing into the cell. Upon solvent being passed into the cell, desorption was rapid and complete. In many cases there was a detectable delay in desorption of the final 0.1 mg m^{-2}. We believe this to be indicative of a minute amount of surfactant which remains strongly electrostatically bound to the surface. This type of behaviour has been observed previously, although not as definitively.[18] Note the consistency of the baseline and in the signal obtained at equilibrium, which suggests that the instrumental error gives an uncertainty in the surface excess of the order of 0.02 mg m^{-2}, nearly an order of magnitude improvement over previous data.

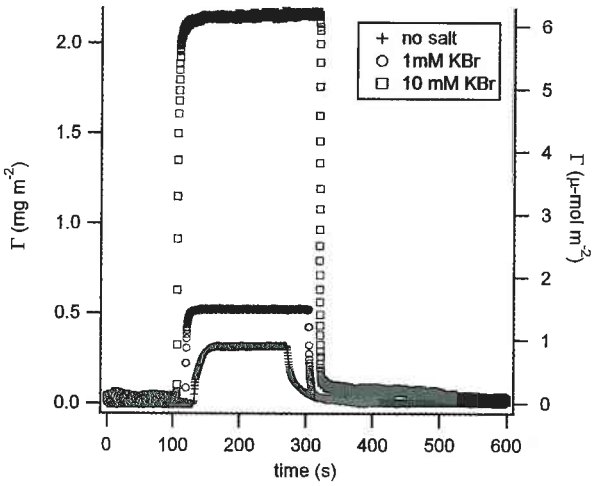

Fig. 2 A selection of typical data showing the adsorption of surfactant in real time measured by optical reflectometry. A stable baseline is recorded before surfactant solution is passed into the cell at approximately 100–120 s. A maximum surface excess is obtained before rinsing the cell with pure solvent again at approximately 300–325 s. In the normal course of experiments much longer time scales were observed.

Apparent adsorption isotherms for CTAB in the absence and presence of both 1 mM and 10 mM KBr produced from data such as that shown in Fig. 2 are presented in Fig. 3 (linear-log)

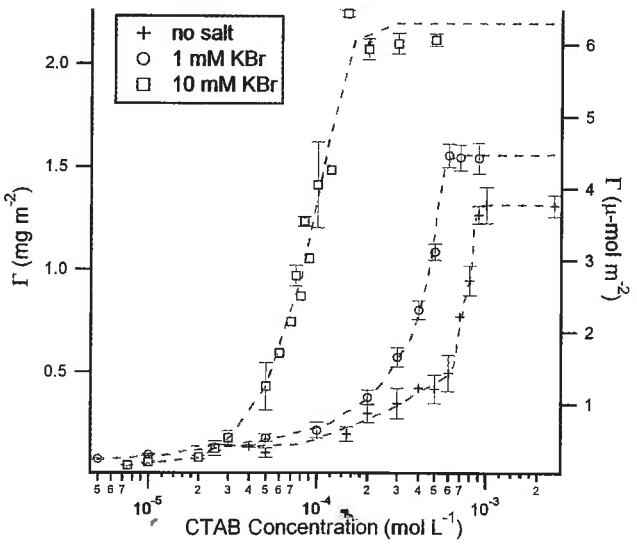

Fig. 3 Apparent adsorption isotherms for CTAB in the absence of salt and in the presence of 1 mM and 10 mM KBr, presented on a linear-log scale. Where error bars are not visible it indicates that the error bars determined from repeat determinations are less than the size of the symbol.

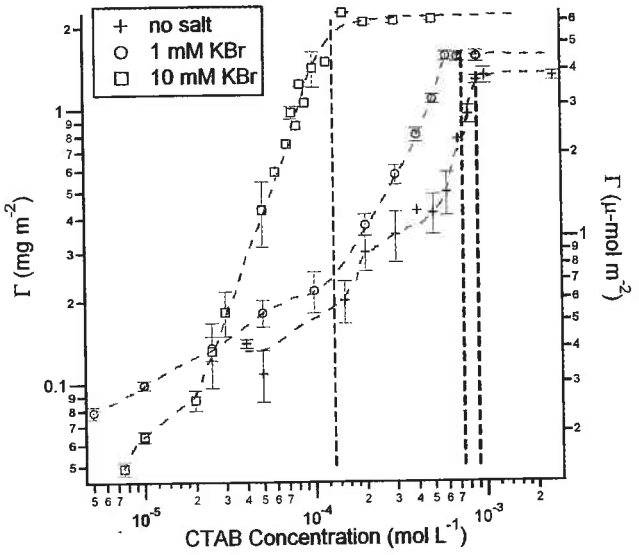

Fig. 4 Apparent adsorption isotherms for CTAB in the absence of salt and in the presence of 1 mM and 10 mM KBr, presented on a log–log scale. Vertical lines indicate cmc for each system. Where error bars are not visible it indicates that the error bars determined from repeat determinations are less than the size of the symbol.

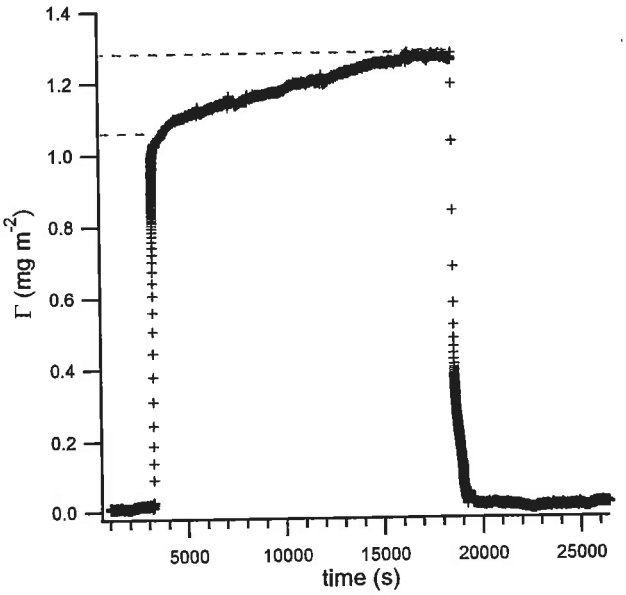

Fig. 5 Adsorption to silica of 0.8 mM CTAB in the absence of salt showing an initial rapid adsorption and then a slow adsorption. A stable baseline was obtained for approximately 1 h, at which time surfactant solution was introduced. The surface excess rapidly rose to approximately 1 mg m^{-2} and gradually increased to 1.28 mg m^{-2} over approximately 4 h. When pure water was reintroduced the system returned to baseline where it remained stable for nearly 2 h.

and 4 (log–log). Dashed lines are presented to guide the eye. All data were collected using optical reflectometry and are consistent with previous reports.[5,12,29] For consistency when constructing the isotherm, the maximum surface excess value was recorded between 120 and 180 s for each concentration. We have reported these measurements as *apparent* isotherms as there is some doubt as to whether the surface excess measured here for part of the isotherm is the true equilibrium surface excess due to the slow kinetics associated with equilibration. We explore this further below.

Previously, slow adsorption had been observed over certain regions of the isotherm and was referred to as the slow adsorption region (SAR).[12,13] In order to more carefully investigate the very slow increase in adsorption that continues long after the initial adsorption process we have developed an optical reflectometer that is both more sensitive and more stable. That is, the noise in the signal is lower and the change in signal due to instrumental drift is greatly reduced. This enables the small changes due to slow adsorption to be followed over long time periods. Slow adsorption was observable over a wide concentration range of CTAB both with and without salt present. In Fig. 5 we provide an example of data that exhibit slow adsorption. The initial rapid adsorption results in a surface excess of 1 mg m^{-2}. The surface excess then rises slowly for a period of nearly 4 h before the surface excess stabilises at 1.28 mg m^{-2}. Upon flushing with water the surface excess rapidly decreases and returns to baseline level. The small disturbances in the signal seen for example at 8000 and 12 000 s are attributed to intensity variation in the laser, perhaps due to mode hopping.

Previous studies found no evidence of slow adsorption for CTAB in the presence of 10 mM electrolyte,[12] with the exception of CTAC (the chloride analogue) in the presence of 10 mM LiCl where slow adsorption was observed.[29] We attribute the difference in our findings to the increased resolution and instrument stability obtained with the new optical reflectometer. The very slow changes in surface excess observed in many cases would have been indistinguishable from baseline drift in the previous data. Fig. 6 illustrates the existence of slow adsorption in the presence of different concentrations of electrolyte. The time scale has been truncated in this figure to highlight the adsorption rates but surface excess continued to increase slowly over extended

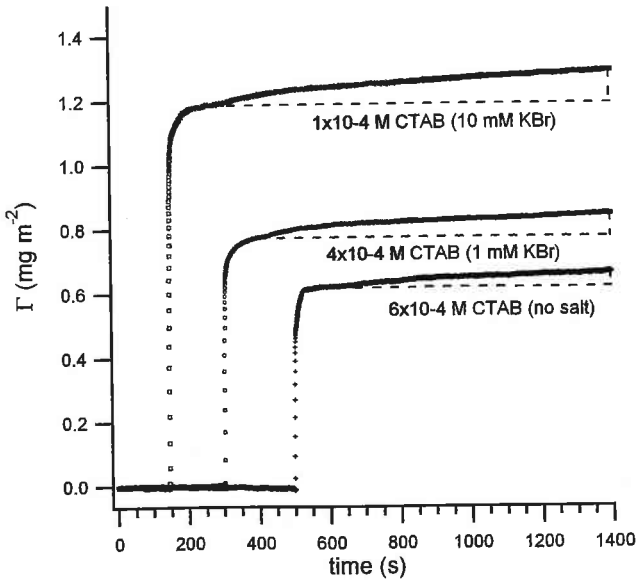

Fig. 6 Three examples of surfactant adsorption highlighting the slow adsorption observed for CTAB in the absence and presence of electrolyte. The time scale has been shifted so that each plot is distinguishable.

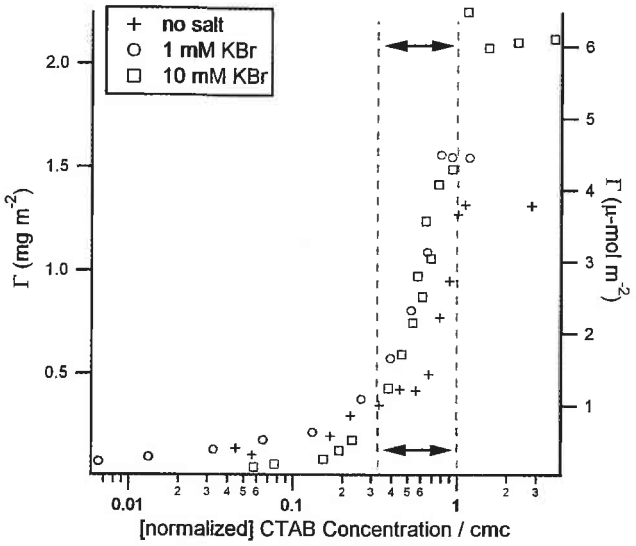

Fig. 7 Normalised isotherms for CTAB in varying levels of electrolyte. The region indicated by arrows indicates the concentration range over which we always observe slow adsorption. The effect has been observed irregularly at lower concentrations and at concentrations around the cmc.

periods of time and always returned to baseline when solvent alone was introduced.

In all cases we find that the initial adsorption process is very rapid and in some cases accounts for the full level of adsorption. This occurs at very low concentrations and at concentrations above the csac. However at other concentrations the initial rapid adsorption is followed by a slow adsorption that can take many hours. The highlighted region of Fig. 7 (normalised isotherm for all three systems) illustrates that slow adsorption occurs over analogous sections of the respective isotherms. While slow adsorption is observed to some degree around the cmc, slow adsorption appears to be absent at very low levels of surface coverage. We note that above the cmc the surface excess is constant. This provides additional evidence that our system does not suffer from gross contamination as any such contaminant would partition into micelles above the cmc and lead to a drop in the measured surface excess.

To quantify this slow increase in surface excess over time, we measured the rate of slow adsorption and found it to be 2–10 × 10^{-5} mg m^{-2} s^{-1} over a series of CTAB concentrations with and without electrolyte. Experimental evidence indicates that the rate of slow adsorption decreases over time but further investigation is necessary to establish this definitively. We wish to explore the origin of this slow adsorption. It has previously been suggested that the hindered kinetics is related to the aggregate structures present at the interface.[5,12] This raises the possibility that for some aggregate structures the adsorption kinetics could become so slow that equilibrium is not reached within reasonable time scales. Indeed a previous experiment has shown evidence of kinetic trapping where the surface excess obtained upon dilution exceeded that obtained when water is displaced with a surfactant solution. This previous attempt to investigate this anomaly was made by utilising a series of sequentially increasing and decreasing concentrations[5] which showed a significant hysteresis in surface excess for CTAB concentrations up to 5 × 10^{-4} M. The data take the form of a stepped pyramid or ziggurat.

With the improved resolution and stability of this new instrumentation we have revisited this experiment for CTAB in the absence of salt, as well as CTAB in the presence of 1 mM and 10 mM KBr, the results of which are summarised in Fig. 8–10. The data presented are raw without any post-processing or reduction. Return to baseline was less than 0.05 mg m^{-2} in the case of CTAB in the absence of salt, and was less than 0.01 mg m^{-2} in the presence of salt. Letters are used to identify bulk solution concentrations during both the increasing and the decreasing sequences. Dashed lines are present to visually highlight the hysteresis in surface excesses for the same concentration between the increasing and decreasing concentration portions of the data (not drawn for all). Without exception, bulk concentrations below the cmc yielded higher surface excess values during the decreasing concentration portion of the cycle. Visual inspection of these differences suggests that the hysteresis is larger for bulk concentrations that lie along the *steep* portion of

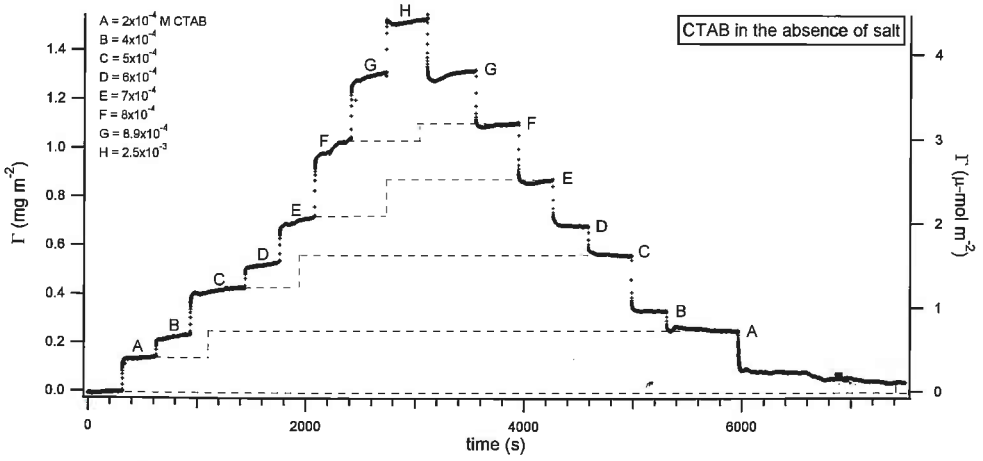

Fig. 8 Concentration cycling (ziggurat) experiment using CTAB in the absence of electrolyte. A stable baseline is obtained before a series of surfactant solutions are introduced to the cell in sequence up to a maximum of 2.5 mM and then repeated in reverse. Letters show solution concentration as indicated by the legend. Dashed lines are present as visual guides to highlight the different surface excesses measured during the up and down cycles.

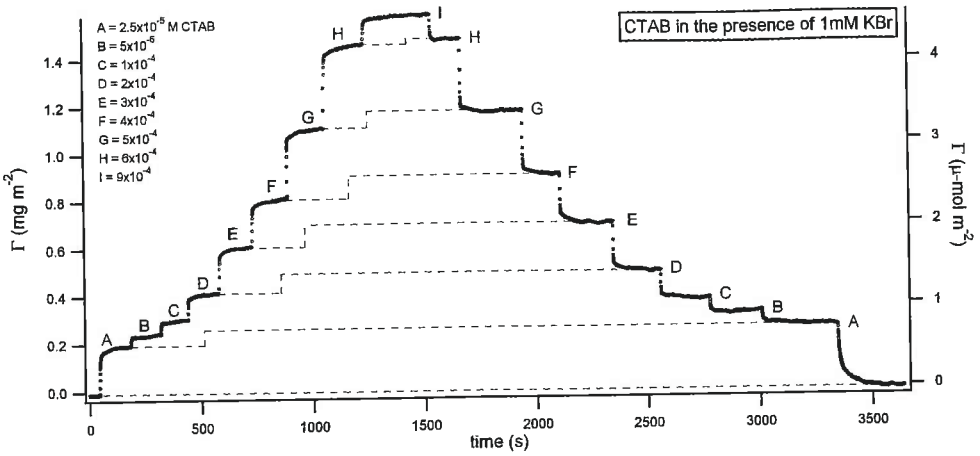

Fig. 9 Concentration cycling (ziggurat) experiment using CTAB in the presence of 1 mM KBr. A stable baseline is obtained before a series of surfactant solutions are introduced to the cell in sequence up to a maximum of 0.9 mM and then repeated in reverse. Letters indicate solution concentration as given by the legend. Dashed lines are present as visual guides to highlight the different surface excesses measured during the up and down cycles.

the respective isotherms. We have included a plot showing the magnitude of the difference as a function of the bulk concentration in the additional material. The magnitude of the difference is generally in the range 0.02–0.2 mg m^{-2}. From this data we can conclude that the surface excess measured in nearly all cases is history dependent. This complicates the determination of the equilibrium surface excess as it is not apparent whether the equilibrium value is obtained upon increasing the concentration, upon dilution or whether it is an intermediate value. Inspection of the data suggests that the surface excess obtained on dilution is more stable with time, supporting the notion that it represents the true equilibrium surface excess.

To further explore this hysteresis in surface excess we performed the same ziggurat experiment using a QCM, the data obtained are shown in Fig. 10. During a QCM measurement the crystal is oscillating in a shear mode. Thus QCM not only provides an alternative means of following the surfactant adsorption process but it was thought possible that the shear wave may provide the necessary energy to overcome the barrier to adsorption and thereby remove the hysteresis in adsorption. Inspection reveals that the hysteresis revealed in the optical reflectometry data is also present in the QCM data, indicating that the shear wave was not able to alter the adsorption kinetics. Silica-coated crystals were used as the most appropriate analogue to substrates used for reflectometry. The surface excess obtained using QCM is routinely higher than that obtained using other techniques due to trapping of water in the film. This water moves with the film and contributes to the decrease in resonant frequency, and thereby registers as an increase in mass. The differences in these measured surface excesses may be used to calculate a mass fraction of water adsorbed with the surfactant at each concentration. Note that injection spikes in the QCM data were removed for clarity as is normal practice, and baseline drift of approximately −0.1 mg m^{-2} was corrected as is common practice (plot of data without baseline correction is provided in ESI†). The presence of injection spikes and the lower signal

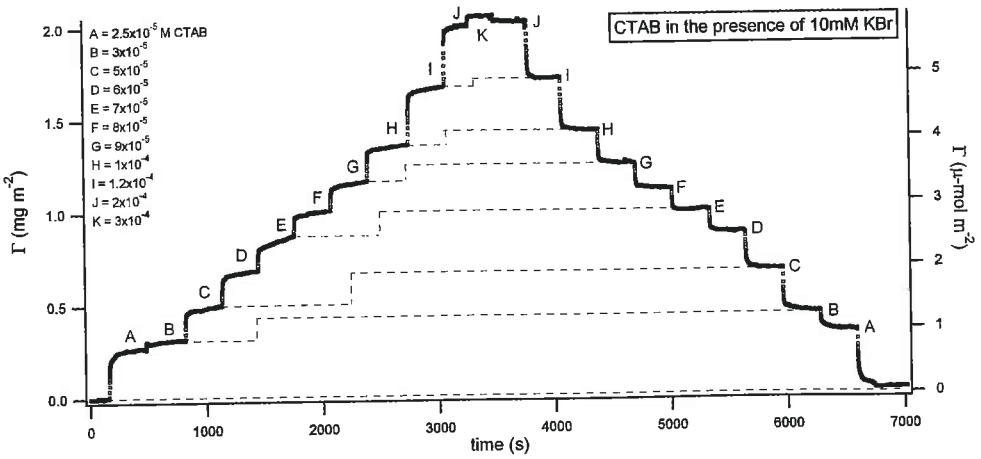

Fig. 10 Concentration cycling (ziggurat) experiment using CTAB in the presence of 10 mM KBr. A stable baseline is obtained before a series of surfactant solutions are introduced to the cell in sequence up to a maximum of 0.3 mM and then repeated in reverse. Letters indicate solution concentration as given by the legend. Dashed lines are present as visual guides to highlight the different surface excesses measured during the up and down cycles.

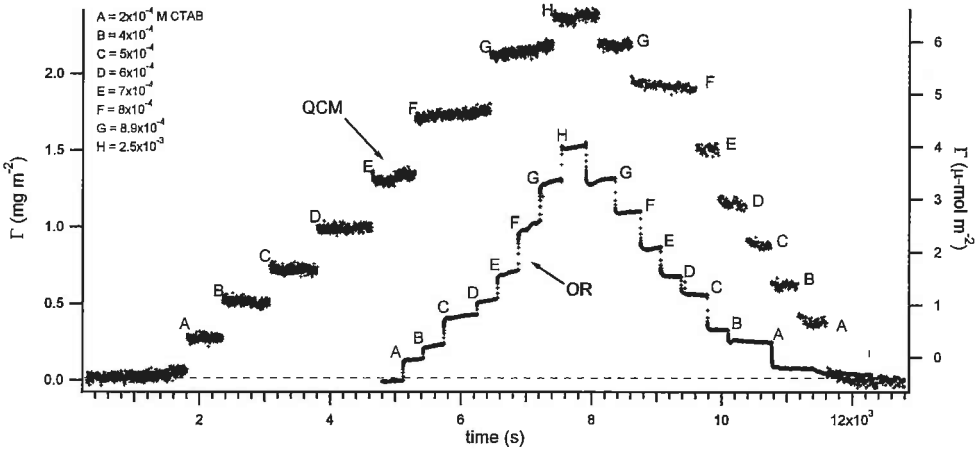

Fig. 11 Concentration cycling experiments in both the OR (repeated from Fig. 8) and the QCM using CTAB in the absence of electrolyte. The same solutions were used for both instruments. Note that injection spikes were removed from QCM data and baseline drift of approximately -0.1 mg m^{-2} was corrected. The same figure without baseline correction is provided in the additional material.

stability obtained when using QCM make it difficult to discern or quantify any type of slow/secondary adsorption regime, but the same hysteresis in surface excess can clearly be discerned in the QCM data.

In an attempt to elucidate some further information about the nature of the adsorbed surfactant layer, we have compared the mass reported by QCM to that reported by OR in Fig. 11 and attributed the difference to water. Again, letters are used to identify the solutions used in each experiment. For illustration we have plotted these water mass fractions on top of the CTAB isotherm in Fig. 12. The data suggest that the least amount of entrained water (65% by mass) is observed for concentrations above the cmc. This is slightly higher than that reported by Penfold *et al.*[30] who divided the surface into two layers and reported 43% and 63% for these layers. We note that the two techniques should not be expected to give identical results as the measure of entrained water obtained by QCM is related to the effective mass and that obtained by optical reflectometry is related to the scattering density. The maximum water fraction measured (130%) occurs at 5×10^{-4} M CTAB, which is 0.55 × cmc or approximately 35% of the maximum surface excess. We note that the nature of the aggregates is not expected to change considerably, rather the density and/or size of the aggregates will increase as the concentration is increased. A possible interpretation of this data is that at surface excesses below the maximum level of entrained water, the density of adsorbed micelles is such that the flow of water is relatively unhindered and at higher coverages the surfactant aggregates begin to fill in the gaps in the adsorbed layer such that less water is entrained by the shearing motion of the crystal. Above the cmc the surfactant layer is most complete and therefore the level of entrained water is at a minimum. Macakova *et al.* recently utilised QCM and OR to study entrained water in several cationic surfactants above the cmc.[27] They measured a mass fraction of water to be 0.42 ± 0.15 for CTAB above the cmc, which is consistent with our result.

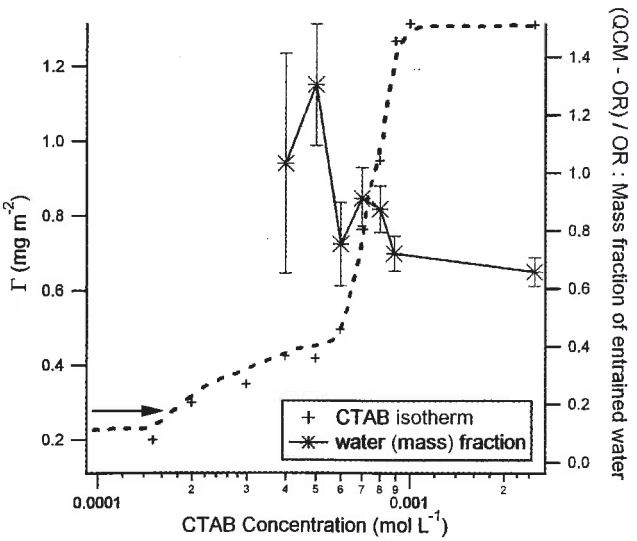

Fig. 12 CTAB isotherm (left scale) plotted alongside mass fraction of entrained water (right scale) as determined by QCM. The mass fraction was calculated as the difference in surface excess as measured by QCM and OR for a given solution. Error bars are calculated by applying the maximum acceptable drift for each instrument and following error propagation.

In addition to frequency, the QCM also measures the dissipation, D, where the dissipation factor is unitless and is defined by $D = E_{\text{dissipated}}/2\pi E_{\text{stored}}$, where $E_{\text{dissipated}}$ is the energy dissipated during one oscillation and E_{stored} is the energy stored in the oscillating system. Inspection of ΔD acquired concurrently with the frequency data indicates that it was, within error, unchanged throughout the experiment and agrees with other published results.[27] This indicates that the film was elastic and is also evidence that the results were not influenced by polymer contamination as adsorbed polymer has a strong influence on ΔD.

The evidence we have provided above, along with earlier AFM observations and previous investigations for C18 surfactants[31] indicate that adsorbed aggregates are not short lived as is widely accepted for micelles in the bulk.[32] Indeed if surface adsorbed aggregates were short lived it is difficult to imagine how slow adsorption could occur or how surface adsorbed aggregates

could be imaged by AFM. This strongly suggests that adsorption at an interface strongly influences the lifetime of an aggregate. Recent work has shown that for CTAB, the adsorbed micelles are symmetrical at all concentrations indicating that many of the micelle bound monomers are not directly interacting with the substrate.[6] It is difficult to see how the monomers facing away from the substrate are influenced strongly by adsorption such that they are micellar bound and the rate of adsorption or desorption is dramatically changed.

The fact that adsorbed aggregates can be imaged by contact mode AFM indicates that surface adsorbed aggregates are immobilised. We propose that the significant factor in increasing the lifetime of the adsorbed aggregates is this immobilisation. Therefore aggregates adsorbed at the interface are unable to collide with other aggregates, except above the cmc where aggregates are also present in solution and these can collide with the surface. This is consistent with the observation that slow adsorption is not seen above the cmc. In a recent study on non-ionic surfactants, Bain[33] has shown that aggregate collision, fusion and subsequent monomer loss is the dominant mechanism by which monomers and micelles equilibrate when near equilibrium. If a similar argument holds for CTAB, then the absence of collisions between aggregates removes the dominant pathway for equilibration of aggregates in the adsorbed layer. Thus during adsorption below the cmc, with aggregate collisions effectively suspended by adsorption, equilibration is dramatically slowed and only occurs through the mechanism of monomer exchange. Far from equilibrium this is effective, but it becomes very slow near equilibrium. The slow adsorption we observe is therefore due to the growth of surface adsorbed aggregates through monomer exchange and the inference is that after the initial rapid adsorption process, the number density of the aggregates on the surface is fixed. That is the increase in surface excess during slow adsorption does not occur by increasing the number of aggregates but by the growth of the aggregates that are already present.

If we accept that the surface adsorbed aggregates are indeed long lived we still have to address the observation that upon dilution the surface excess rapidly drops to baseline levels. When a system is perturbed far from equilibrium the exchange of monomers between adsorbed micelles and solution leads to a rapid approach to equilibrium. Thus in our experiments, when we introduce solvent the system is pushed far from equilibrium and the exchange of monomer between aggregates and the solution is dominated by loss of monomers from the aggregate and the equilibrium with the solvent is restored rapidly. That is, all the surfactant is removed from the surface rapidly.

The observation of slow adsorption kinetics and the hysteresis observed in the ziggurat plots raise the question as to what the true equilibrium level of surface excess is. At this stage we cannot give a definitive answer as it is possible that equilibrium is approached slowly from both directions. However we can state that the increasing and decreasing portions of the ziggurat data provide lower and upper limits to the true equilibrium surface excess. Further, inspection of the data in Fig. 8–10 suggests that the data in the dilution portion are more constant. This suggests that this data are closer to the true equilibrium value. A corollary of the mechanism proposed above is that as equilibrium is approached the rate of change in surface excess diminishes. This suggests that the true equilibrium value could be determined from careful analysis of adsorption kinetics.

Conclusion

In this paper we have shown evidence for a period of secondary (slow) adsorption for CTAB at the silica–water interface. This effect is observed both in the absence and in the presence of electrolyte. Our work suggests that surface adsorbed aggregates are long lived and the slow adsorption kinetics is due to their lack of translational freedom, this removes micelle–micelle collisions from the equilibration process. Equilibration therefore takes place through monomer exchange between the solution and the surface. The slow adsorption measured reflects the fact that this process is slow when equilibrium is approached. A series of concentration and dilution experiments were conducted which confirm previous reports regarding hysteresis in adsorbed surface excess, and suggest that the amount of material adsorbed on the surface is highly dependent on the history of that surface and hence there is some uncertainty in the true values of equilibrium surface excess. However the concentration and dilution measurements provide upper and lower bounds on the true equilibrium value. These indicate that the uncertainty is greatest in the steepest portion of the adsorption isotherms. Comparison of QCM and OR data suggests that entrained water is significant in the adsorption of CTAB and is highest at 0.45 × cmc, or about 35% of the maximum surface excess. The proposed mechanism should apply to surfactants of all types and suggests that slow adsorption and therefore the associated problems in determining the true surface excess may be a universal phenomenon.

Acknowledgements

We would like to thank Prof. Colin Bain for fruitful discussions of his work related to surfactant adsorption and bulk micellar behaviour, which contributed to the development of this article. We would also like to thank Dr Erica Wanless for the generous donation of the silicon oxide substrates with controlled oxide layer thickness. SCH gratefully acknowledges financial support from the Smartprint CRC and the American Australian Association. VSJC gratefully acknowledges financial support from the Australian Research Council and the International Fine Particle Research Institute.

References

1 Y. Gao, J. Du and T. Gu, *J. Chem. Soc., Faraday Trans. 1*, 1987, **83**, 2671–2679.
2 H. M. Rendall and D. B. Hough, in *Adsorption from Solutions at the Solid–Liquid Interface*, ed. G. D. Parfitt and C. H. Rochester, Academic Press, London, 1983, ch. 1.
3 P. Somasundaran and D. W. Fuerstenau, *J. Phys. Chem.*, 1966, **70**, 90–96.
4 S. Manne, J. P. Cleveland, H. E. Gaub, G. D. Stucky and P. K. Hansma, *Langmuir*, 1994, **10**, 4409–4413.
5 R. Atkin, V. S. J. Craig, E. J. Wanless and S. Biggs, *Adv. Colloid Interface Sci.*, 2003, **103**, 219–304.
6 E. Tyrode, M. W. Rutland and C. D. Bain, *J. Am. Chem. Soc.*, 2008, **130**, 17434–17445.
7 W. A. Ducker and E. J. Wanless, *Langmuir*, 1999, **15**, 160–168.
8 E. J. Wanless, T. W. Davey and W. A. Ducker, *Langmuir*, 1997, **13**, 4223–4228.

9 E. J. Wanless and W. A. Ducker, *J. Phys. Chem.*, 1996, **100**, 3207–3214.
10 B. D. Fleming, E. J. Wanless and S. Biggs, *Langmuir*, 1999, **15**, 8719–8725.
11 S. B. Velegol, B. D. Fleming, S. Biggs, E. J. Wanless and R. D. Tilton, *Langmuir*, 2000, **16**, 2548–2556.
12 R. Atkin, V. S. J. Craig and S. Biggs, *Langmuir*, 2000, **16**, 9374–9380.
13 R. Atkin, V. S. J. Craig and S. Biggs, *Langmuir*, 2001, **17**, 6155–6163.
14 T. J. Senden, personal communication.
15 R. K. Iler, *The Chemistry of Silica*, Wiley-Interscience Publishers, New York, 1979.
16 J. C. Dijt, M. A. C. Stuart, J. E. Hofman and G. J. Fleer, *Colloids Surf.*, 1990, **51**, 141–158.
17 R. M. A. Azzam, in *Ellipsometry and Polarized Light*, ed. R. M. A. Azzam and N. M. Bashara, North-Holland Pub. Co., Amsterdam, 1987, ch. 4.
18 R. Atkin, PhD thesis, University of Newcastle, 2002.
19 E. S. Pagac, D. C. Prieve and R. D. Tilton, *Langmuir*, 1998, **14**, 2333–2342.
20 F. Caruso, T. Serizawa, D. N. Furlong and Y. Okahata, *Langmuir*, 1995, **11**, 1546–1552.
21 F. Höök, B. Kasemo, T. Nylander, C. Fant, K. Sott and H. Elwing, *Anal. Chem.*, 2001, **73**, 5796–5804.
22 G. M. Liu, J. P. Zhao, Q. Y. Sun and G. Z. Zhang, *J. Phys. Chem. B*, 2008, **112**, 3333–3338.
23 G. M. Liu, S. R. Zou, L. Fu and G. Z. Zhang, *J. Phys. Chem. B*, 2008, **112**, 4167–4171.
24 M. A. Plunkett, P. M. Claesson and M. W. Rutland, *Langmuir*, 2002, **18**, 1274–1280.
25 P. Roach, D. Farrar and C. C. Perry, *J. Am. Chem. Soc.*, 2005, **127**, 8168–8173.
26 G. Sauerbrey, *Z. Phys.*, 1959, **155**, 206–222.
27 L. Macakova, E. Blomberg and P. M. Claesson, *Langmuir*, 2007, **23**, 12436–12444.
28 V. S. J. Craig and M. Plunkett, *J. Colloid Interface Sci.*, 2003, **262**, 126–129.
29 R. Atkin, V. S. J. Craig, E. J. Wanless and S. Biggs, *J. Colloid Interface Sci.*, 2003, **266**, 236–244.
30 G. Fragneto, R. K. Thomas, A. R. Rennie and J. Penfold, *Langmuir*, 1996, **12**, 6036–6043.
31 J. Zhang, R. H. Yoon, M. Mao and W. A. Ducker, *Langmuir*, 2005, **21**, 5831–5841.
32 E. A. G. Aniansson and S. N. Wall, *J. Phys. Chem.*, 1974, **78**, 1024–1030.
33 C. D. Bain, personal communication.